Supplementary Materials for

Crude Oil Impairs Cardiac Excitation-Contraction Coupling in Fish

Fabien Brette, Ben Machado, Caroline Cros, John P. Incardona, Nathaniel L. Scholz, Barbara A. Block*

*Corresponding author. E-mail: bblock@stanford.edu

This PDF file includes

Materials and Methods

Fish Origin and Care

Pacific bluefin (fish mass = 11.7 ± 1.0 kg, heart mass = 43.2 ± 3.4 g, mean ± SEM, n = 40) and yellowfin tunas (fish mass = 7.7 ± 1.9 kg, heart mass = 20.2 ± 1.8 g, mean ± SEM, n = 17) were captured in the California Current and held aboard the *F/V Shogun* in seawater wells, and transported by truck to the Tuna Research and Conservation Center (Pacific Grove, CA). Tunas were held in a 109-m^3 tank at 20 ± 1°C and fed a diet of squid, sardines, and enriched gelatin, as previously described (*34, 35*). Fish were acclimated for periods of at least 4-8 weeks at 20°C. All procedures were in accordance with Stanford IACUC protocols.

Cardiomyocyte Isolation

Cardiomyocytes were obtained by enzymatic isolation using a protocol previously described (*24*). Briefly, fish were pithed and the heart was excised and perfused (7.5 mL/min) with isolating solution until it had stopped beating and was clear of blood. This was accomplished by retrograde perfusion through the ventricular lumen for ~ 20 min. The coronary artery was cannulated with PE-50 tubing and a 60 ml syringe containing isolation solution was used to perfuse the blood from the arteries and compact myocardial tissue. Proteolytic enzymes were then added to the isolating solution, and retrograde luminal perfusion was continued for ~ 50 minutes. After enzymatic treatment, the atrium and ventricle were placed in separate dishes containing fresh isolating solution at ~ 20°C. Tissues were cut into small pieces with scissors and then triturated through the opening of a Pasteur pipette to free individual myocytes. Freshly isolated myocytes were stored in the isolation solution for up to 8 h at 20°C. All experiments were performed at room temperature (20 ± 1°C).

Physiological Solutions

The isolating solution contained (in mM) 100 NaCl, 10 KCl, 1.2 KH_2PO_4, 4 $MgSO_4$, 50 taurine, 20 glucose, and 10 HEPES, with pH adjusted to 6.9 with NaOH at 20 °C. For

enzymatic digestion, collagenase (type IA, 0.75 mg/mL), trypsin (type IX, 0.25 mg/mL), and fatty acid-free BSA (0.75 mg/mL) were added to this solution.

The composition of the extracellular physiological solution (Ringer) was based on a previous study (30) and contained (in mM) 150 NaCl, 5.4 KCl, 1.5 $MgCl_2$, 3.2 $CaCl_2$, 10 glucose and 10 HEPES, pH set to 7.7 with NaOH. This solution was used for action potential and intracellular $[Ca^{2+}]$ measurements. To avoid overlapping currents, the extracellular physiological solution was modified for K^+ current (I_K) and Ca^{2+} (I_{Ca}) recordings. For I_K recording, tetrodotoxin (TTX, 0.5 µM), nifedipine (10 µM), and glibenclamide (10 µM) were included in the Ringer solution to inhibit Na^+, Ca^{2+}, and ATP-sensitive K^+ channels respectively. For I_{Ca} measurement, KCl was replaced by CsCl to inhibit K^+ channels, and in some experiments TTX (1 µM) was added to block Na^+ channels.

Pipette solutions were optimized for each electrophysiological recording for tunas based on previous studies (26, 36). For action potential measurement, pipette solution contained (in mM): 10 NaCl, 140 KCl, 5 MgATP, 0.025 EGTA, 1 $MgCl_2$, and 10 HEPES, pH adjusted to 7.2 with KOH. The low concentration of EGTA was included to achieve near physiological Ca^{2+} buffering capacity. For I_K measurement, pipette solution contained (in mM): 10 NaCl, 140 KCl, 5 MgATP, 5 EGTA, 1 $MgCl_2$, and 10 HEPES, pH adjusted to 7.2 with KOH. The high concentration of EGTA was included to block Na^+-Ca^{2+} exchanger current. For I_{Ca}, the pipette solution contained (in mM) 130 CsCl, 15 TEA-Cl, 5 MgATP, 1 $MgCl_2$, 5 Na_2-phosphocreatine, 0.025 EGTA, 10 HEPES, and 0.03 Na_2GTP, pH adjusted to 7.2 with CsOH. The low concentration of EGTA was included to achieve near physiological Ca^{2+} buffering capacity. CsCl and TEA-Cl were included to inhibit K^+ currents.

Oils samples and WAF preparation

All oil samples were collected under chain of custody during the DWH oil spill response effort. Samples used in toxicity assays included: riser oil (sample 072610-03, "Source"), riser oil that was artificially weathered by slow heating at 90-105 ºC until the volume was reduced by 20% to produce artificially weathered-riser (sample 072610-W-A,

"Weathered"), and a surface Slick A (sample CTC02404-02), collected 29 July 2010 from a barge holding mixed oil offloaded from a number of different skimmers; and a second surface Slick B (sample GU2888-A0719-OE701), collected from a skimming transect completed 19 July 2010 by the U.S. Coast Guard Cutter *Juniper*. High-energy WAFs were prepared using a commercial stainless steel blender as previously described (*37*) at 1000 ppm, and filtered to remove oil droplets. For each oil preparation, a sample of the "stock" WAF solution used in the electrophysiological experiments was sent to Columbia Analytical Services (CAS; Kelso, WA) for analytical chemistry to confirm PAHs exposure concentrations. Serial dilutions solutions (20%, 10%, 5%) were used in physiological experiments to determine the concentration-response relationship for oil cardiotoxicity. Total ($\sum$) PAH concentrations are given in Table S1. All concentrations given on figures are expressed as $\sum$PAHs (in µg/liter) for each specific oil sample. Negative controls (*i.e.* background concentration of PAHs) were obtained by using the same WAF protocol, using Ringer solution but without MC252 DWH oil; mean value was 1.33 ± 0.16 µg/L total PAHs (n = 45). Isolated cardiomyocytes were exposed to $\sum$PAH concentrations at the lower end of 1) the range previously shown to cause cardiotoxicity in demersal fish embryos (10) and 2) the range of $\sum$PAHs measured in some water samples during the Deepwater Horizon spill (e.g., up to 84.8 µg/L (17)), the latter expected to yield proportionally higher tissue concentrations in relatively smaller pelagic embryos.

Electrophysiological recordings
Cardiomyocytes were studied in a chamber mounted on the stage of an inverted microscope (Nikon Diaphot, Japan). Cells were initially superfused with Ringer solution. Membrane potential and ion channel currents were recorded in the whole-cell configuration of the patch clamp technique using settings and properties appropriate for cardiomyocytes (*29*). Briefly, an Axopatch 200B (Axon Instruments, CA) amplifier was controlled by a Pentium PC connected via a Digidata 1322A A/D converter (Axon Instruments, CA), which was used also for data acquisition and analysis using pClamp software (Axon Instruments, CA). Signals were filtered at 1-10 kHz using an 8-pole Bessel low pass filter before digitization at 10-20 kHz and storage. Patch pipette resistance was typically 1.5-3 MΩ when filled with intracellular solution (above). Cell

3

membrane capacitance was measured using the "membrane test module" in Clampex (fitting the decay of the capacitance current recorded during a 10 mV depolarizing pulse from a holding potential of -80 mV). At the beginning of each trial, cardiomyocytes were loaded onto the perfusing chamber, allowed to settle for ~10 minutes, and then perfused with control external solution. Membrane potentials and currents were recorded from each myocyte under baseline (control) conditions, and then recorded again across an increasing series of WAF concentrations in the extracellular solution.

Action potentials were stimulated (evoked) using 10 ms sub-threshold current steps at a frequency of 0.5 Hz. K^+ current (I_K) was measured using an established protocol adapted from previous studies on Pacific bluefin tuna (26) and rainbow trout (38). I_K was activated by a pre-pulse to +40 mV (to fully activate K^+ channels) and was then measured as the tail current at -20 mV, the maximum tail current in tuna cardiomyocytes (26). The voltage waveform for this protocol is shown in Figure 2. To separate rapid K^+ current (I_{Kr}), tail I_K amplitude was measured as the current sensitive to a specific I_{Kr} inhibitor (2 μM E-4031). Trains of depolarizing pulses were applied 0.2 Hz every 20 seconds. In a second set of experiments, current-voltage (I-V) relationships were obtained by holding the myocytes at -80 mV and stepping to -70 to +40 mV (10 mV step) for 4 sec and then stepping back to -20 mV to obtain a tail current.

Ca^{2+} current (I_{Ca}) was elicited by a pulse to 0 mV (~peak of the current-voltage relationship in cardiomyocytes) after a pre-pulse to -40 mV to inactivate Na^+ current. I_{Ca} was measured as the difference between the peak and the end of pulse current. In a second set of experiments, current-voltage relationships were obtained by holding the myocytes at -80 mV and stepping to -70 to +50 mV (10 mV step) for 300 ms. To block Na^+ current, 1 μM TTX was added to the external solution. I_{Ca} was also elicited by a representative action potential waveform. The action potential waveforms were the average of the action potentials recorded in the current clamp experiments in cardiomyocytes in control Ringer and cardiomyocytes after perfusion of Slick B at 5% WAF dilution (n = 7). Trains of depolarizing pulses were applied at 0.2 Hz.

4

<u>Intracellular [Ca^{2+}] measurements.</u>

Confocal Ca^{2+} imaging was performed using a laser-scanning unit attached to an Olympus inverted microscope. Control and WAF-treated cardiomyocytes were loaded with 4 µM Fluo-4 AM (Molecular Probes) for 20 min, then perfused with standard Ringer. The dye was excited with the 488 nm line of an argon laser and fluorescence measured at > 500 nm. Transverse line scans were acquired at 5 ms intervals. Cells were electrically stimulated at 0.5 Hz via extracellular electrodes. Some cells were also incubated with sarcoplasmic reticulum inhibitors (5 µM ryanodine and 2 µM thapsigargin) for at least 30 minutes. Batches of cardiomyocytes were incubated with WAFs for at least 1 hour.

<u>Data analysis</u>

Data analysis was performed using Clampfit (Axon Instruments, CA) and Origin (OriginLab Corporation, MA) software. For action potentials, the resting membrane potential (RMP), action potential amplitude (APA), and action potential duration (APD) at three different percentages of repolarization (10: APD_{10}; 50: APD_{50}; 90: APD_{90}, respectively) were analyzed. Triangulation is defined as the repolarization time from APD_{30} to APD_{90} (Triang30-90) (*18*). Control experiments showed that these parameters were stable over the time of recording (<10 min). Concentration-response curves (Figure S4) were fit to a logistic equation by use of a Marquardt-Levenburg algorithm for least-squares nonlinear regression analysis.

Currents are expressed as current density (pA/pF). I_K amplitude was measured as the current sensitive to E-4031. I_{Ca} was measured as the difference between the peak inward current and the current at the end of the depolarizing pulse. Because the decay of I_{Ca} varied between cell types and experimental conditions, the kinetics of inactivation of I_{Ca} were characterized by the time required for the current to decay to 0.37 of the peak amplitude ($T_{0.37}$) (*39*). I_{Ca} was also analyzed by integrating I_{Ca} during the test pulse to obtain total Ca^{2+} influx. Ca^{2+} entry is expressed as charge density (fC/pF).

Ca^{2+} transients from confocal experiments were analyzed using Image J, Clampfit and Origin. At least three traces at steady state were analyzed and averaged. The decay of

5

Ca^{2+} transient was fitted by a single exponential decay to calculate Tau of decay (*i.e.* time to decrease to 37% of the peak amplitude). The amplitude of the Ca^{2+} transient is defined as peak increase and basal Ca^{2+} (F/F0) (*40*). Ca^{2+} transients were filtered off-line at 10 Hz (*41*).

Chemicals

All solutions were prepared using ultrapure water supplied by a Milli-Q system (Millipore, USA). All chemicals were reagent grade and purchased from Sigma (St. Louis, MO) except for TTX (Tocris, UK), Ryanodine (Ascent Scientific, MA), Fluo-4 (Molecular Probes, NY) and E-4031 (Enzo Life Sciences, NY).

Statistics

Data are presented as mean ± S.E.M. Statistical analysis was performed using SigmaStat software (Systat Software, CA). For electrophysiological data, One Way Repeated Measures Analysis of Variance (after confirmation of normal distribution and equal variance) was used; otherwise, Friedman Repeated Measures Analysis of Variance on Ranks followed by a Student-Newman-Keuls test for post hoc analysis were used. For confocal data, unpaired t-test was used. $P < 0.05$ was considered significant.
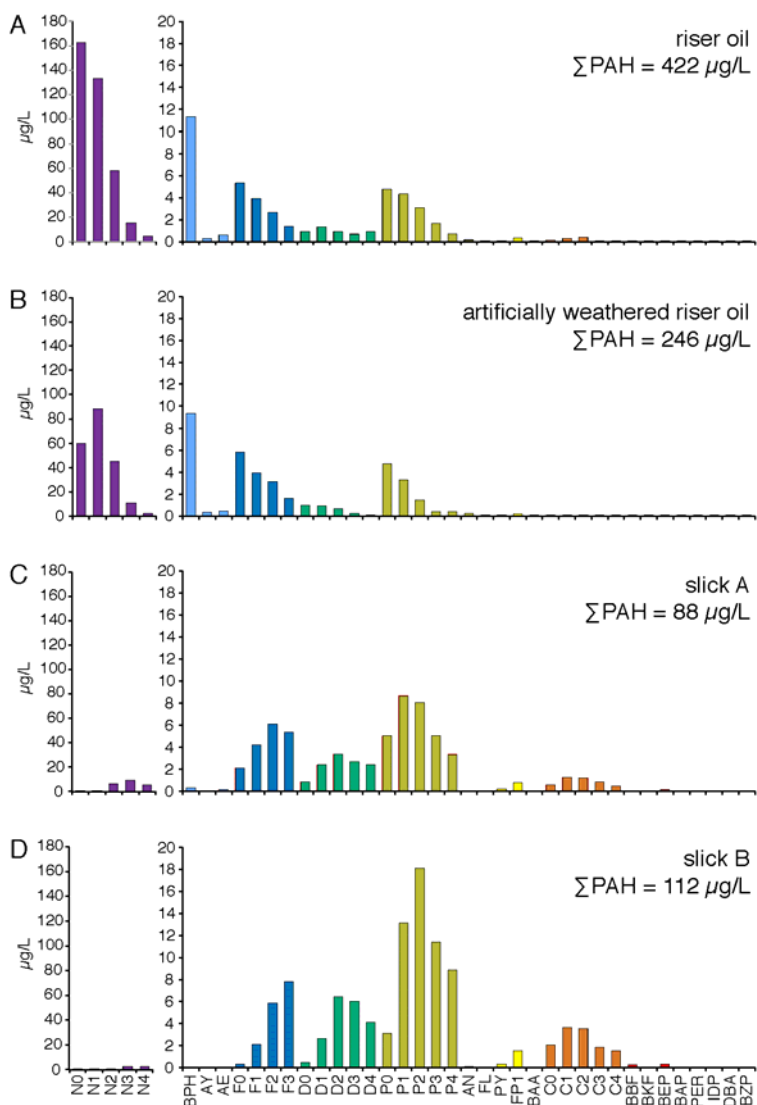
Fig. S1: PAHs concentrations in four WAFs.

Values represent single measurements from riser oil (Source), artificially weathered riser oil (Weathered) Slick A, and Slick B. N, naphthalenes; AY, acenaphthylene; AE, acenaphthene; F, fluorene; D, dibenzothiophene; P, phenanthrene; AN, anthracene; FL, fluoranthene; PY, pyrene; FP, fluoranthenes/pyrenes; BAA, benz[*a*]anthracene; C, chrysene; BBF, benzo[*b*]fluoranthene; BKF, benzo[*j*]fluoranthene/benzo[*k*]fluoranthene; BEP, benzo[e]pyrene; BAP, benzo[a]pyrene; PER, perylene; IDP, indeno[1,2,3-*cd*]pyrene, DBA, dibenz[*a,h*]anthracene/dibenz[*a,c*]anthracene; BZP, benzo[*ghi*]perylene. Parent compound is indicated by a 0 (e.g., N0), while numbers of additional carbons (e.g. methyl groups) for alkylated homologs are indicated as N1, N2, etc.

7
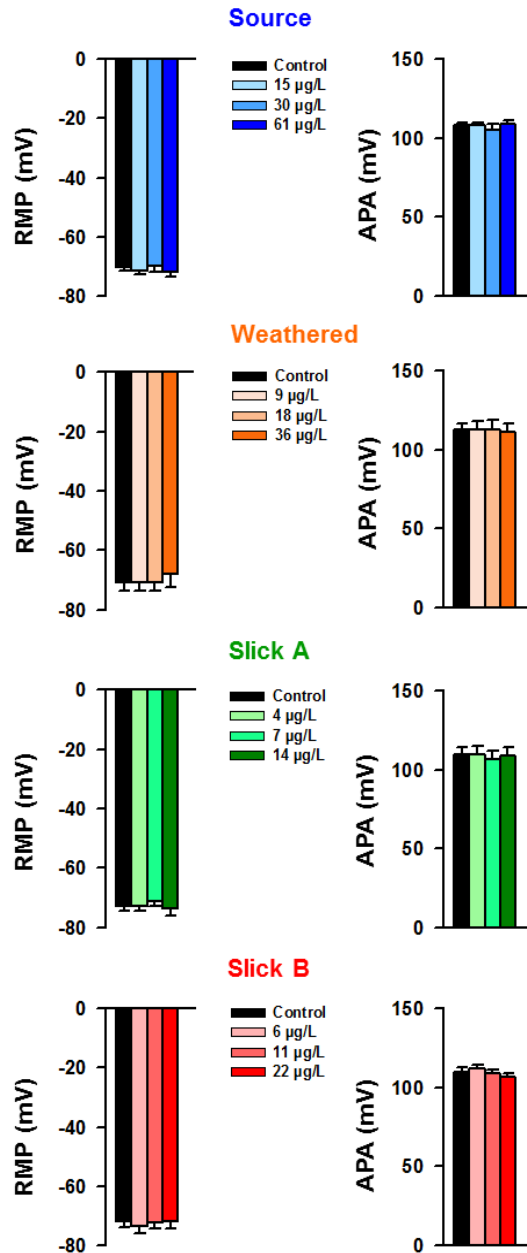
Fig. S2: Effect of oil WAFs on resting membrane potential and action potential amplitude in bluefin tuna ventricular cardiomyocytes.

Mean ± SEM of resting membrane potential (RMP) and action potential amplitude (APA) recorded in control condition (black bars) and in ascending concentrations of Source (blue bars), Weathered (orange bars), Slick A (green bars) and Slick B (red bars) WAFs, respectively, n = 9 for Source, 8 for Weathered, 7 for Slick A and 7 for Slick B experiments.
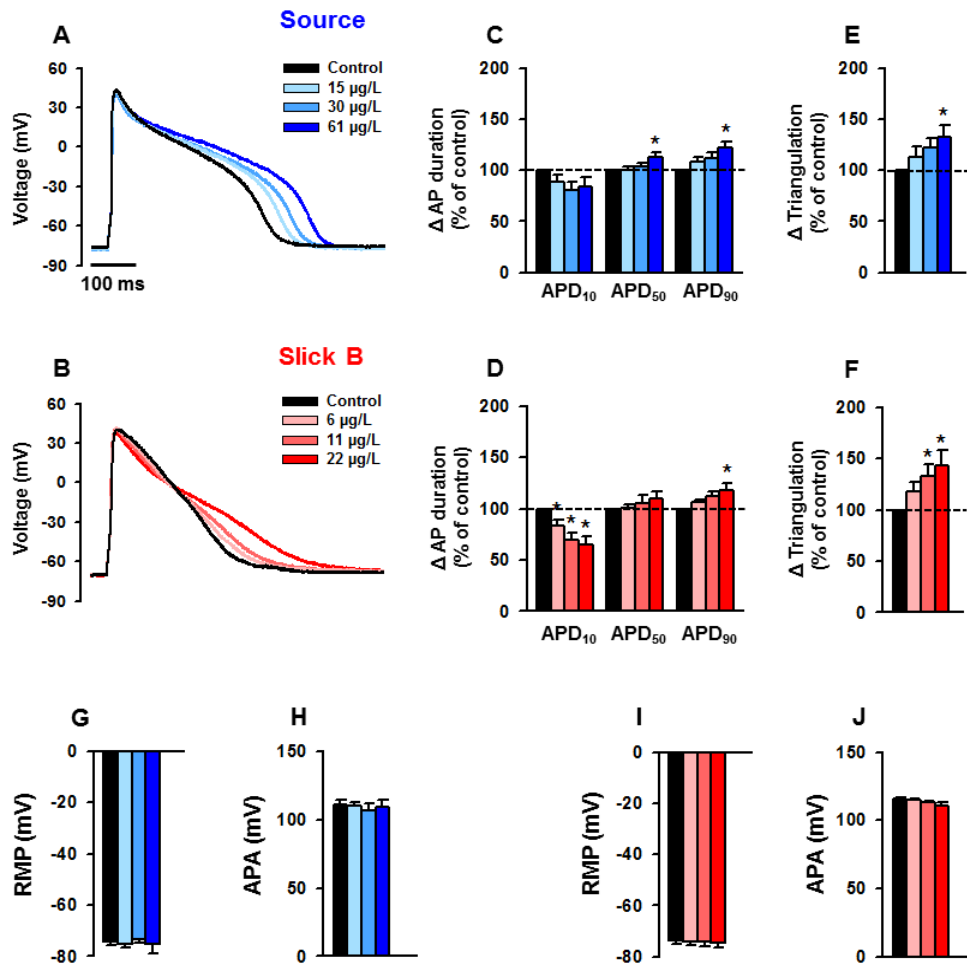
Fig. S3: Effect of oil WAFs on action potential characteristics from yellowfin tuna ventricular cardiomyocytes.

A-B: Action potentials recorded in control condition (black traces) and in the presence of ascending concentrations of Source (blue traces, **A**) and Slick B WAFs (red traces, **B**). **C-D:** Mean ± SEM of action potential duration (APD, expressed as % of control) at 10, 50 and 90% repolarization in control condition (black bars) and in ascending concentrations of Source (blue bars, **C**) and Slick B (red bars, **D**). **E-F:** Mean ± SEM of action potential triangulation (expressed as % of control; calculated as $APD_{90}-APD_{30}$) in control (black bars) and with ascending concentrations of Source (blue bars, **E**) and Slick B (red bars, **F**). **G-J:** Mean ± SEM of resting membrane potential (RMP) and action potential amplitude (APA) in control (black bars) and after application of ascending concentrations of Source (blue bars, **G** and **H**; respectively) and Slick B (red bars, **I** and **J**; respectively), n = 7 for Source and 7 for Slick B experiments. * indicates $P < 0.05$.
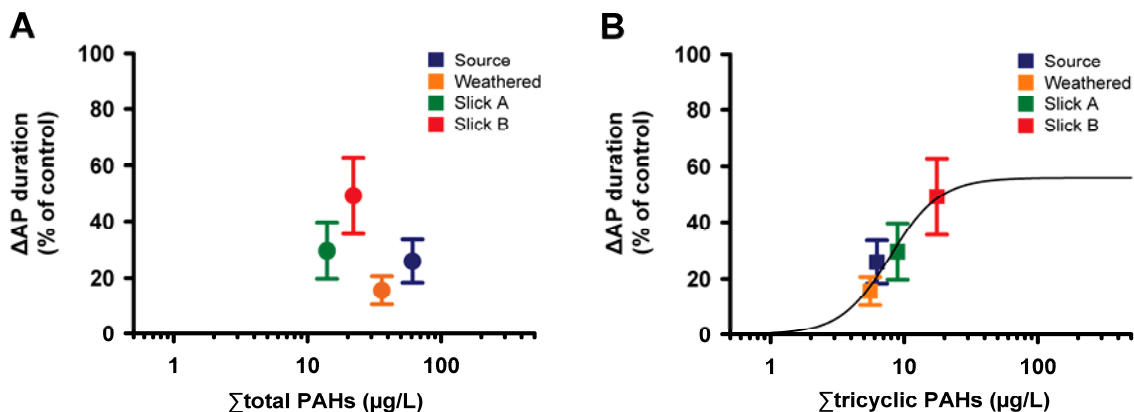
Fig. S4: Relationship between ΔAP duration and ∑PAHs.

A: Mean ± SEM data for ΔAP duration following WAF exposures expressed as a function of ∑total PAHs. Note that no logistic fit can be performed, indicating no relation between ΔAP duration and ∑total PAHs. **B:** Mean ± SEM data for ΔAP duration following WAF exposures expressed as a function of ∑tricyclic PAHs. Note that the data can be fitted with a logistic (R^2=0.9), indicating a clear dose-dependence between ΔAP duration and ∑tricyclic PAHs (EC_{50} = 7.8 ± 5.1 µg/L). Data from action potential recordings (APD_{90}) from bluefin tuna cardiomyocytes (Figure 1) with WAFs at 20% dilution (Table S1).
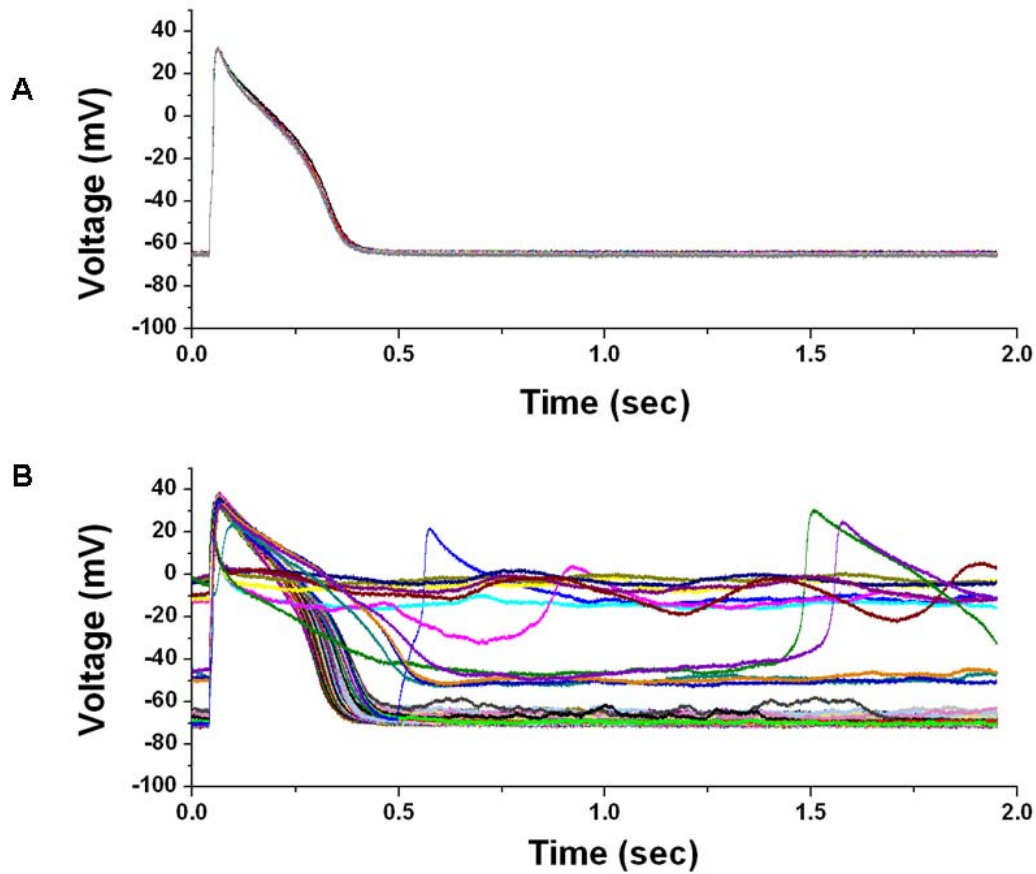
Fig. S5: Cellular arrhythmia in bluefin tuna ventricular cardiomyocytes in response to increasing concentrations of Slick B WAF on action potential.

A: Typical recording of successive action potentials (~20 traces stacked) from a bluefin tuna cardiomyocyte in control physiological solution. Note that the traces show little difference, indicating stability of recording **B:** Action potentials in response to an increasing concentration of Slick B WAF (ΣPAH: from 0 to 22 µg/L). Note that WAF exposure initially prolongs the action potential and then induces cellular arrhythmia.
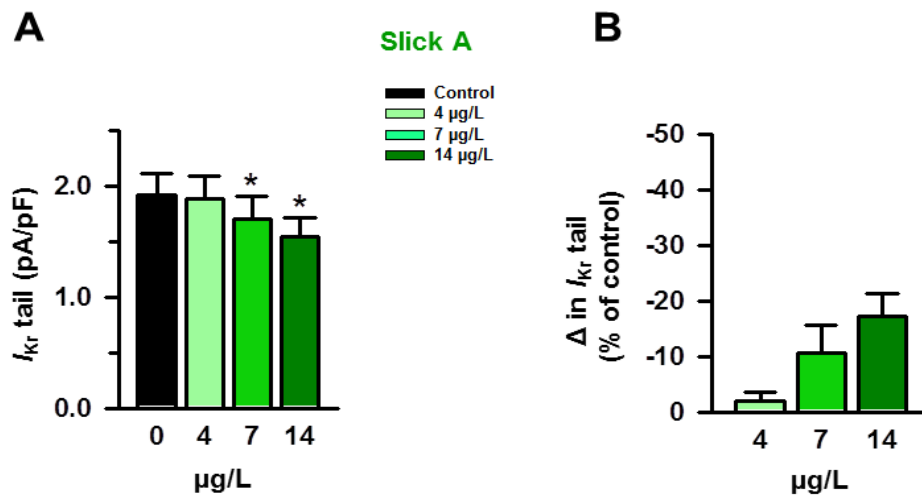
Fig. S6: Effect of oil WAF (Slick A) on K$^+$ current (I_{Kr}) from bluefin tuna ventricular cardiomyocytes.

A: Mean ± SEM of tail I_{Kr} in control (black bars) and in presence of ascending concentrations of Slick A WAF (green bars). **B:** Mean ± SEM of change in I_{Kr} tail (expressed as % of control) with ascending concentrations of Slick A (green bars), n = 8. * indicates $P < 0.05$.
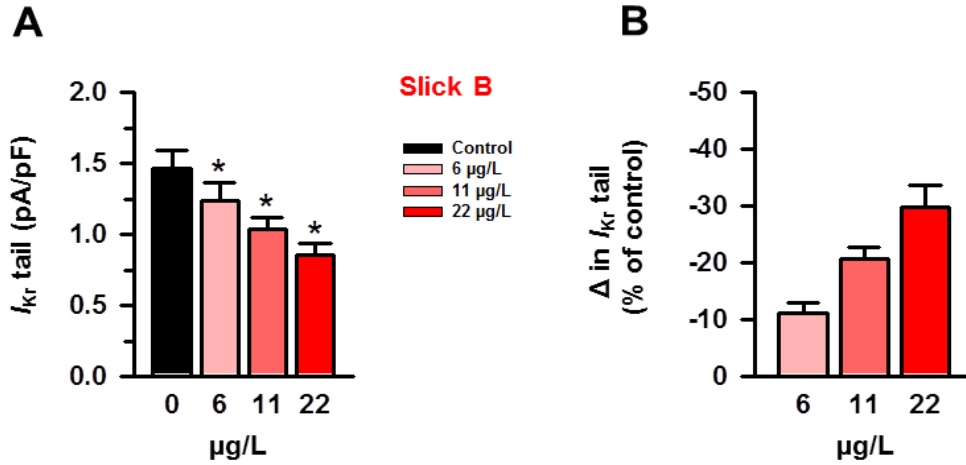
**Fig. S7: Effect of oil WAF (Slick B) on K$^+$ current (I_{Kr}) from yellowfin ventricular cardiomyocytes.**

A: Mean ± SEM of tail I_{Kr} (black bars) and in the presence of ascending concentrations of Slick B WAF (red bars). **B:** Mean ± SEM of change in I_{Kr} tail (expressed as % of control) in response to concentrations of WAF Slick B (red bars), n = 9. * indicates $P < 0.05$.
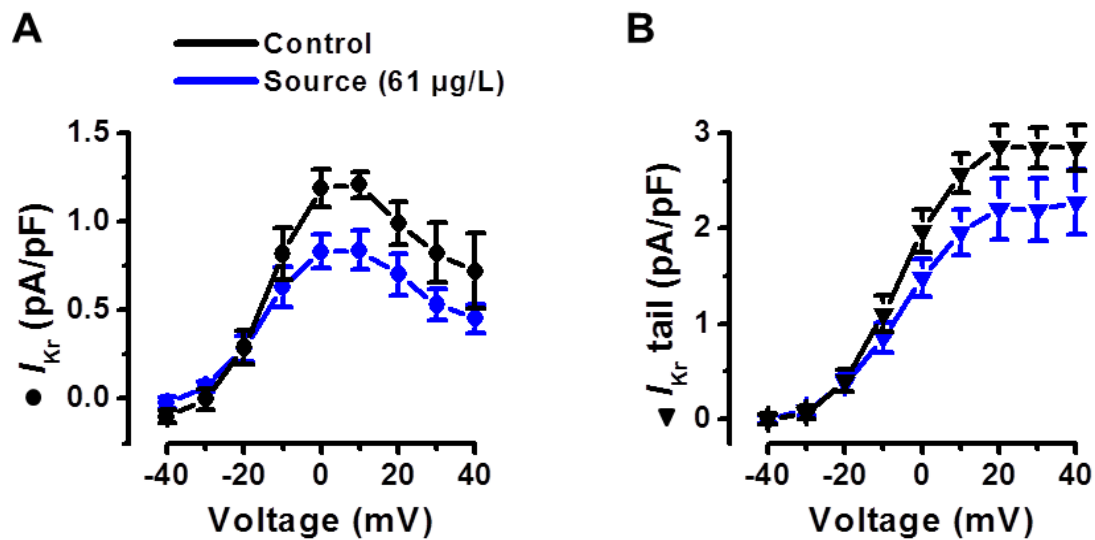
Fig. S8: Effect of oil WAF (Source) on K$^+$ current (I_{Kr}) from bluefin tuna ventricular cardiomyocytes.

A-B: Mean ± SEM of current-voltage relationship of I_{Kr} (circle, **A**) and tail I_{Kr} (triangle, **B**) in control (black trace) and in the presence of Source WAF (61 μg/L, blue trace), n = 6.
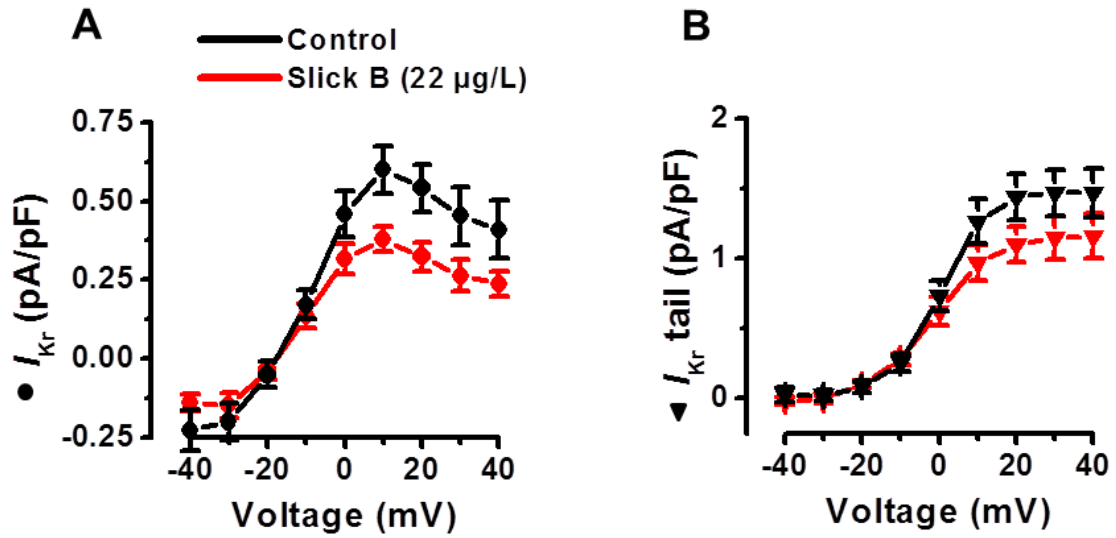
Fig. S9: Effect of oil WAF (Slick B) on K^{+} current (I_{Kr}) from yellowfin ventricular cardiomyocytes.

A-B: Mean ± SEM of current-voltage relationship of I_{Kr} (circle, **A**) and tail I_{Kr} (triangle, **B**) in control (black trace) and with Slick B WAF (22 µg/L, red trace), n = 8.
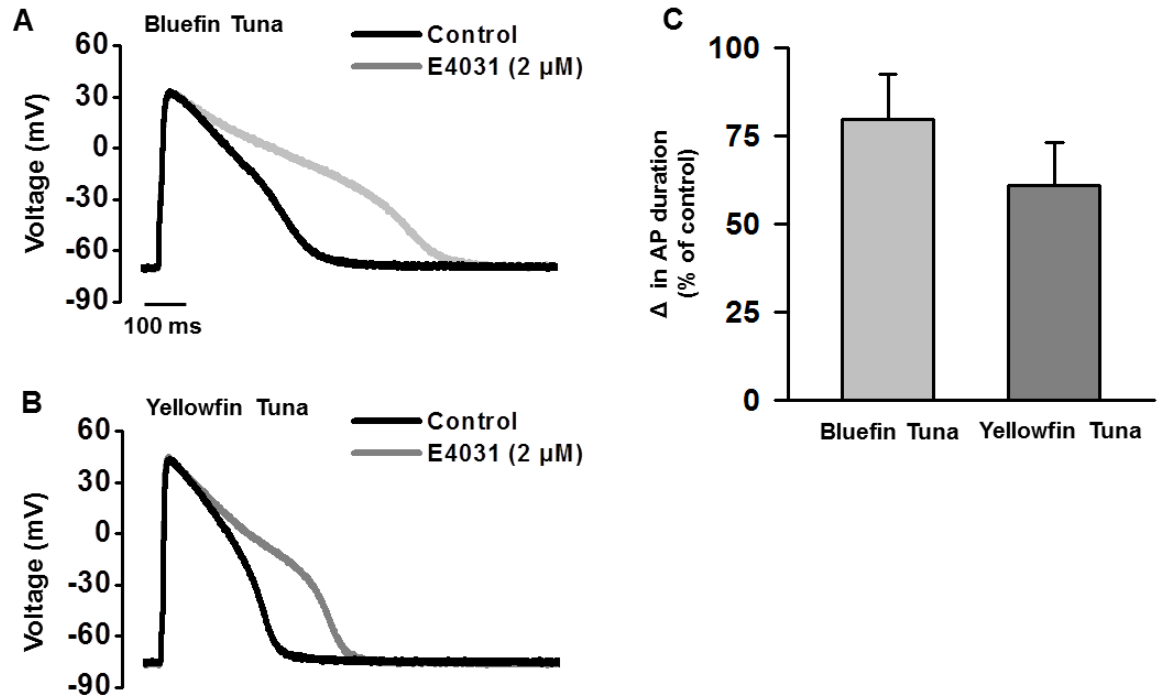
Fig. S10: Effect of E4031 action potential duration from bluefin and yellowfin tuna ventricular cardiomyocytes.

A-B: Action potentials in control condition (black) and with I_K blocker E4031 (2 μM, grey trace) in bluefin tuna (**A**) and yellowfin tuna (**B**) ventricular myocytes. **C:** Mean ± SEM change in AP duration (expressed as % of control) in bluefin tuna (light grey bar) and yellowfin tuna (dark grey bar), n = 6 for both species.
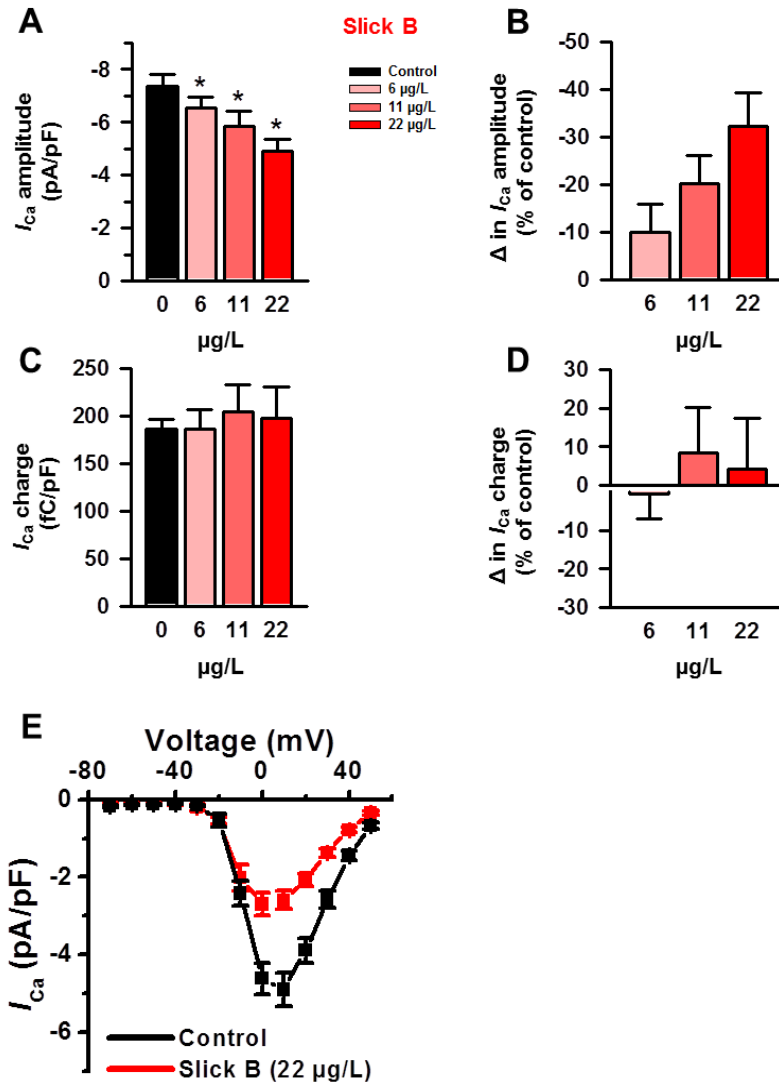
Fig. S11: Effect of oil WAF (Slick B) on Ca^{2+} current (I_{Ca}) from yellowfin ventricular cardiomyocytes.

A: Mean ± SEM of I_{Ca} amplitude in control (black bars) and in the presence of ascending concentrations of Slick B WAF (red bars). **B:** Mean ± SEM of change in I_{Ca} amplitude (expressed as % of control) with ascending concentrations of Slick B (red bars). **C:** Mean ± SEM of I_{Ca} charge in control (black bars) and in the presence of ascending concentrations of WAF (red bars). **D:** Mean ± SEM of change in I_{Ca} charge (expressed as % of control) with ascending concentrations of WAF Slick B (red bars), n = 5. **E:** Mean ± SEM of current-voltage relationship of I_{Ca} in control (black trace) and in presence of Slick B (22 µg/L, red trace), n = 6. * indicates $P < 0.05$.
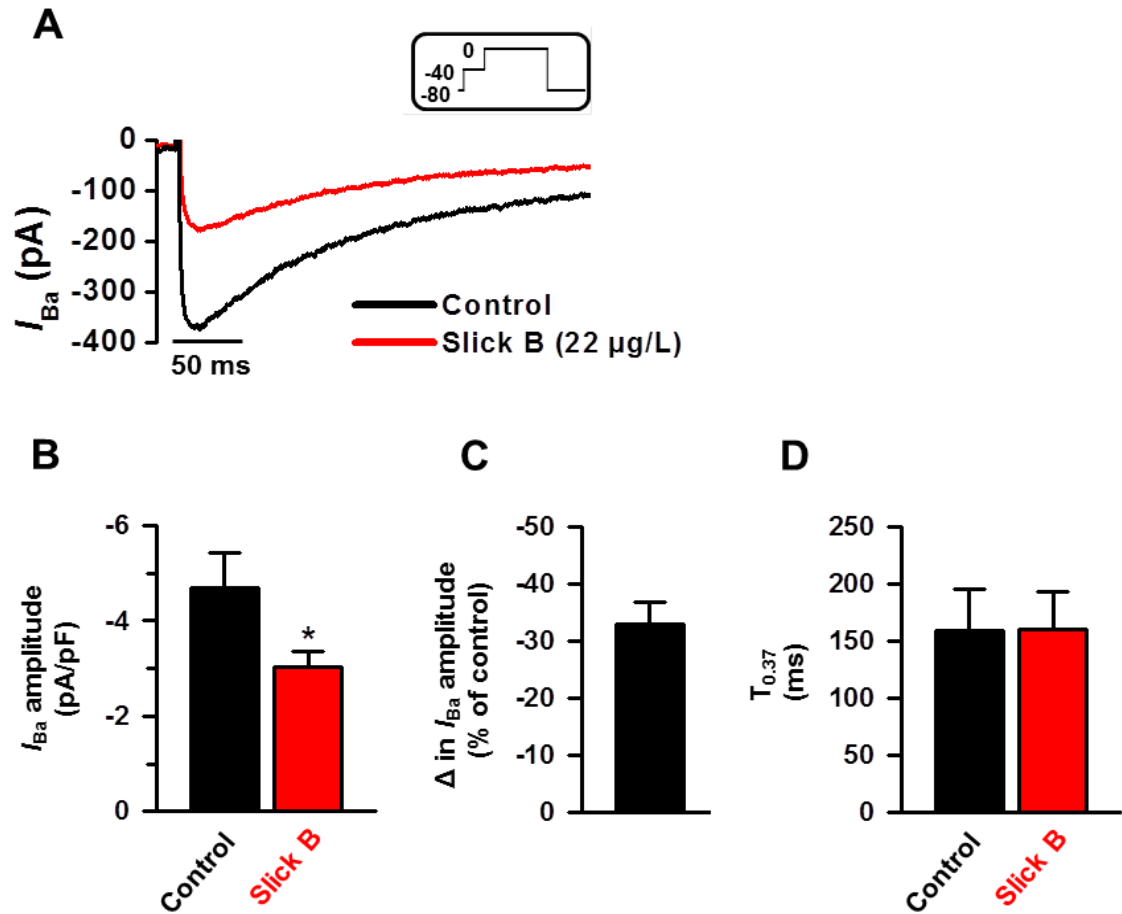
Fig. S12: Effect of oil WAF (Slick B) on Ba^{2+} current (I_{Ba}) from bluefin tuna ventricular cardiomyocytes.

A: I_{Ba} recorded in control condition (black trace) and with Slick B WAF (22 µg/L, red trace). **Inset:** Voltage step to record I_{Ba}. **B:** Mean ± SEM of I_{Ba} amplitude in control (black bar) and with Slick B (22 µg/L, red trace). **C.** Mean ± SEM of change in I_{Ba} amplitude (expressed as % of control). **D.** Mean ± SEM time to decline to 37% of I_{Ba} peak (T$_{0.37}$) in control (black bar) and with Slick B (22 µg/L, red trace). Data from n = 6 cells. * indicates $P < 0.05$.
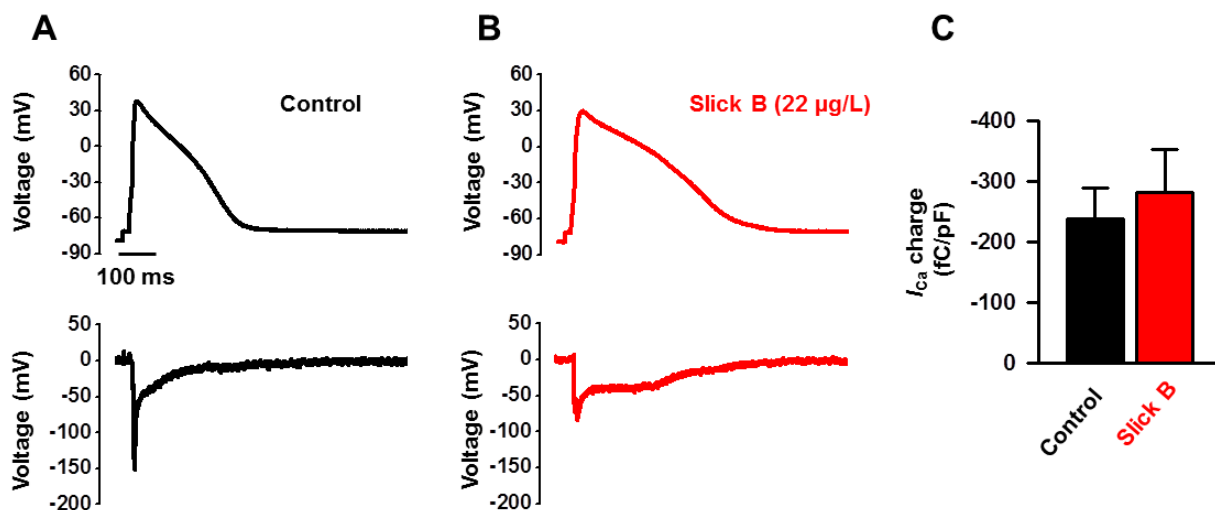
Fig. S13: Effect of WAF oil (Slick B) on Ca^{2+} current (I_{Ca}) recorded in action potential clamp from bluefin tuna ventricular cardiomyocytes.

A-B: Action potential clamp and the associated I_{Ca} recorded in control condition (black trace, **A**) and with Slick B WAF (22 µg/L, red trace, **B**). **C:** Mean ± SEM of I_{Ca} charge in control (black bar) and with Slick B (22 µg/L, red trace), n = 5.
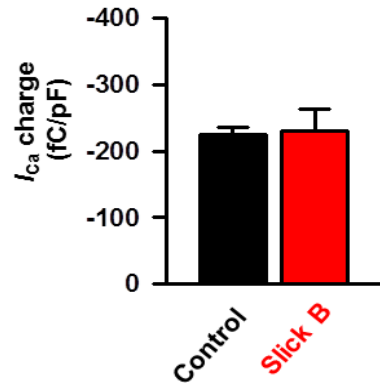
Fig. S14: Effect of WAF oil (Slick B) on Ca^{2+} current (I_{Ca}) during action potential clamp from yellowfin ventricular cardiomyocytes.

Mean ± SEM of I_{Ca} charge during action potential clamp protocol in control (black bar) and with Slick B WAF (22 µg/L, red trace), n = 6. * indicates $P < 0.05$.

Table S1. Average PAH concentrations in WAFs. ∑PAHs data are means ± SEM measured in all WAF stocks (1000 ppm mass oil load). ∑Tricyclic PAHs include the 3-ringed parent and alkylated fluorenes, dibenzothiophenes and phenanthrenes. Diliution values derived from the first column (1000 ppm mass oil load).

Oil	∑PAHs (µg/L)	∑Tricyclic PAHs (µg/L)	∑PAHs (µg/L)		
			20% dilution	10% dilution	5% dilution
Source (n = 14)	303.3 ± 22.8	31.2 ± 3.7	60.7	30.3	15.2
Weathered (n = 6)	179.0 ± 20.5	27.8 ± 1.3	35.8	17.9	9.0
Slick A (n = 8)	71.0 ± 5.5	44.6 ± 4.8	14.2	7.1	3.6
Slick B (n = 25)	111.7 ± 5.8	87.7 ± 5.0	22.3	11.2	5.6

References

1. M. G. Carls, J. P. Meador, A perspective on the toxicity of petrogenic PAHs to developing fish embryos related to environmental chemistry. *Hum. Ecol. Risk Assess. Int. J.* **15**, 1084–1098 (2009). doi:10.1080/10807030903304708

2. C. H. Peterson, S. D. Rice, J. W. Short, D. Esler, J. L. Bodkin, B. E. Ballachey, D. B. Irons, Long-term ecosystem response to the Exxon Valdez oil spill. *Science* **302**, 2082–2086 (2003). doi:10.1126/science.1084282 Medline

3. C. E. Boström, P. Gerde, A. Hanberg, B. Jernström, C. Johansson, T. Kyrklund, A. Rannug, M. Törnqvist, K. Victorin, R. Westerholm, Cancer risk assessment, indicators, and guidelines for polycyclic aromatic hydrocarbons in the ambient air. *Environ. Health Perspect.* **110** (suppl. 3), 451–488 (2002). doi:10.1289/ehp.02110s3451 Medline

4. J. J. Stegeman, J. J. Lech, Cytochrome P-450 monooxygenase systems in aquatic species: Carcinogen metabolism and biomarkers for carcinogen and pollutant exposure. *Environ. Health Perspect.* **90**, 101–109 (1991). doi:10.2307/3430851 Medline

5. J. P. Incardona, C. A. Vines, B. F. Anulacion, D. H. Baldwin, H. L. Day, B. L. French, J. S. Labenia, T. L. Linbo, M. S. Myers, O. P. Olson, C. A. Sloan, S. Sol, F. J. Griffin, K. Menard, S. G. Morgan, J. E. West, T. K. Collier, G. M. Ylitalo, G. N. Cherr, N. L. Scholz, Unexpectedly high mortality in Pacific herring embryos exposed to the 2007 Cosco Busan oil spill in San Francisco Bay. *Proc. Natl. Acad. Sci. U.S.A.* **109**, E51–E58 (2012). doi:10.1073/pnas.1108884109 Medline

6. M. G. Carls, S. D. Rice, J. E. Hose, Sensitivity of fish embryos to weathered crude oil: Part I. Low-level exposure during incubation causes malformations, genetic damage, and mortality in larval pacific herring (*Clupea pallasi*). *Environ. Toxicol. Chem.* **18**, 481 (1999).

7. R. A. Heintz, J. W. Short, S. D. Rice, Sensitivity of fish embryos to weathered crude oil: Part II. Increased mortality of pink salmon (*Oncorhynchus gorbuscha*) embryos incubating downstream from weathered *Exxon Valdez* crude oil. *Environ. Toxicol. Chem.* **18**, 494 (1999).

8. J. P. Incardona, T. K. Collier, N. L. Scholz, Defects in cardiac function precede morphological abnormalities in fish embryos exposed to polycyclic aromatic hydrocarbons. *Toxicol. Appl. Pharmacol.* **196**, 191–205 (2004). doi:10.1016/j.taap.2003.11.026 Medline

9. J. P. Incardona, M. G. Carls, H. Teraoka, C. A. Sloan, T. K. Collier, N. L. Scholz, Aryl hydrocarbon receptor-independent toxicity of weathered crude oil during fish development. *Environ. Health Perspect.* **113**, 1755–1762 (2005). doi:10.1289/ehp.8230 Medline

10. J. P. Incardona, M. G. Carls, H. L. Day, C. A. Sloan, J. L. Bolton, T. K. Collier, N. L. Scholz, Cardiac arrhythmia is the primary response of embryonic Pacific herring (*Clupea pallasi*) exposed to crude oil during weathering. *Environ. Sci. Technol.* **43**, 201–207 (2009). doi:10.1021/es802270t Medline

11. J. H. Jung, C. E. Hicken, D. Boyd, B. F. Anulacion, M. G. Carls, W. J. Shim, J. P. Incardona, Geologically distinct crude oils cause a common cardiotoxicity syndrome in developing zebrafish. *Chemosphere* **91**, 1146–1155 (2013). doi:10.1016/j.chemosphere.2013.01.019 Medline

12. J. P. Incardona, T. K. Collier, N. L. Scholz, Oil spills and fish health: Exposing the heart of the matter. *J. Expo. Sci. Environ. Epidemiol.* **21**, 3–4 (2011). doi:10.1038/jes.2010.51 Medline

13. J. D. Neilson, S. E. Campana, A validated description of age and growth of western Atlantic bluefin tuna (*Thunnus thynnus*). *Can. J. Fish. Aquat. Sci.* **65**, 1523–1527 (2008). doi:10.1139/F08-127

14. B. A. Block, S. L. Teo, A. Walli, A. Boustany, M. J. Stokesbury, C. J. Farwell, K. C. Weng, H. Dewar, T. D. Williams, Electronic tagging and population structure of Atlantic bluefin tuna. *Nature* **434**, 1121–1127 (2005). Medline doi:10.1038/nature03463

15. J. R. Rooker, J. R. Simms, R. J. Wells, S. A. Holt, G. J. Holt, J. E. Graves, N. B. Furey, Distribution and habitat associations of billfish and swordfish larvae across mesoscale features in the Gulf of Mexico. *PLoS ONE* **7**, e34180 (2012). doi:10.1371/journal.pone.0034180 Medline

16. Materials and methods are available as supplementary materials on *Science* Online.

17. A. R. Diercks, R. C. Highsmith, V. L. Asper, D. J. Joung, Z. Zhou, L. Guo, A. M. Shiller, S. B. Joye, A. P. Teske, N. Guinasso, T. L. Wade, S. E. Lohrenz, Characterization of subsurface polycyclic aromatic hydrocarbons at the Deepwater Horizon site. *Geophys. Res. Lett.* **37**, n/a (2010). doi:10.1029/2010GL045046

18. L. M. Hondeghem, L. Carlsson, G. Duker, Instability and triangulation of the action potential predict serious proarrhythmia, but action potential duration prolongation is antiarrhythmic. *Circulation* **103**, 2004–2013 (2001). doi:10.1161/01.CIR.103.15.2004 Medline

19. J. M. Nerbonne, R. S. Kass, Molecular physiology of cardiac repolarization. *Physiol. Rev.* **85**, 1205–1253 (2005). doi:10.1152/physrev.00002.2005 Medline

20. P. Kannankeril, D. M. Roden, D. Darbar, Drug-induced long QT syndrome. *Pharmacol. Rev.* **62**, 760–781 (2010). doi:10.1124/pr.110.003723 Medline

21. D. M. Bers, Cardiac excitation-contraction coupling. *Nature* **415**, 198–205 (2002). doi:10.1038/415198a Medline

22. M. B. Cannell, H. Cheng, W. J. Lederer, The control of calcium release in heart muscle. *Science* **268**, 1045–1049 (1995). doi:10.1126/science.7754384 Medline

23. H. A. Shiels, E. V. Freund, A. P. Farrell, B. A. Block, The sarcoplasmic reticulum plays a major role in isometric contraction in atrial muscle of yellowfin tuna. *J. Exp. Biol.* **202**, 881–890 (1999). Medline

24. H. A. Shiels, A. Di Maio, S. Thompson, B. A. Block, Warm fish with cold hearts: Thermal plasticity of excitation-contraction coupling in bluefin tuna. *Proc. Biol. Sci.* **278**, 18–27 (2011). doi:10.1098/rspb.2010.1274 Medline

25. M. Vornanen, H. A. Shiels, A. P. Farrell, Plasticity of excitation-contraction coupling in fish cardiac myocytes. *Comp. Biochem. Physiol. A Mol. Integr. Physiol.* **132**, 827–846 (2002). doi:10.1016/S1095-6433(02)00051-X Medline

26. G. L. Galli, M. S. Lipnick, B. A. Block, Effect of thermal acclimation on action potentials and sarcolemmal K$^+$ channels from Pacific bluefin tuna cardiomyocytes. *Am. J. Physiol. Regul. Integr. Comp. Physiol.* **297**, R502–R509 (2009). doi:10.1152/ajpregu.90810.2008 Medline

27. F. Brette, J. Leroy, J. Y. Le Guennec, L. Sallé, Ca^{2+} currents in cardiac myocytes: Old story, new insights. *Prog. Biophys. Mol. Biol.* **91**, 1–82 (2006). doi:10.1016/j.pbiomolbio.2005.01.001 Medline

28. F. Brette, G. Luxan, C. Cros, H. Dixey, C. Wilson, H. A. Shiels, Characterization of isolated ventricular myocytes from adult zebrafish (*Danio rerio*). *Biochem. Biophys. Res. Commun.* **374**, 143–146 (2008). doi:10.1016/j.bbrc.2008.06.109 Medline

29. F. Brette, L. Sallé, C. H. Orchard, Quantification of calcium entry at the T-tubules and surface membrane in rat ventricular myocytes. *Biophys. J.* **90**, 381–389 (2006). doi:10.1529/biophysj.105.069013 Medline

30. H. A. Shiels, E. White, Temporal and spatial properties of cellular Ca^{2+} flux in trout ventricular myocytes. *Am. J. Physiol. Regul. Integr. Comp. Physiol.* **288**, R1756–R1766 (2005). doi:10.1152/ajpregu.00510.2004 Medline

31. H. Tie, B. D. Walker, C. B. Singleton, S. M. Valenzuela, J. A. Bursill, K. R. Wyse, S. N. Breit, T. J. Campbell, Inhibition of HERG potassium channels by the antimalarial agent halofantrine. *Br. J. Pharmacol.* **130**, 1967–1975 (2000). doi:10.1038/sj.bjp.0703470 Medline

32. C. E. Hicken, T. L. Linbo, D. H. Baldwin, M. L. Willis, M. S. Myers, L. Holland, M. Larsen, M. S. Stekoll, S. D. Rice, T. K. Collier, N. L. Scholz, J. P. Incardona, Sublethal exposure to crude oil during embryonic development alters cardiac morphology and reduces aerobic capacity in adult fish. *Proc. Natl. Acad. Sci. U.S.A.* **108**, 7086–7090 (2011). doi:10.1073/pnas.1019031108 Medline

33. J. M. Blank, J. M. Morrissette, A. M. Landeira-Fernandez, S. B. Blackwell, T. D. Williams, B. A. Block, In situ cardiac performance of Pacific bluefin tuna hearts in response to acute temperature change. *J. Exp. Biol.* **207**, 881–890 (2004). doi:10.1242/jeb.00820 Medline

34. J. M. Blank, J. M. Morrissette, C. J. Farwell, M. Price, R. J. Schallert, B. A. Block, Temperature effects on metabolic rate of juvenile Pacific bluefin tuna *Thunnus orientalis*. *J. Exp. Biol.* **210**, 4254–4261 (2007). doi:10.1242/jeb.005835 Medline

35. C. J. Farwell, 10. Tunas in captivity. *Fish Physiol.* **19**, 391–412 (2001). doi:10.1016/S1546-5098(01)19011-4

36. G. L. Galli, M. S. Lipnick, H. A. Shiels, B. A. Block, Temperature effects on Ca^{2+} cycling in scombrid cardiomyocytes: A phylogenetic comparison. *J. Exp. Biol.* **214**, 1068–1076 (2011). doi:10.1242/jeb.048231 Medline

37. J. P. Incardona, T. L. Swarts, R. C. Edmunds, T. L. Linbo, A. Aquilina-Beck, C. A. Sloan, L. D. Gardner, B. A. Block, N. L. Scholz, Exxon Valdez to Deepwater Horizon: Comparable toxicity of both crude oils to fish early life stages. *Aquat. Toxicol.* **142-143**, 303–316 (2013). doi:10.1016/j.aquatox.2013.08.011 Medline

38. M. Vornanen, A. Ryökkynen, A. Nurmi, Temperature-dependent expression of sarcolemmal K($^+$) currents in rainbow trout atrial and ventricular myocytes. *Am. J. Physiol. Regul. Integr. Comp. Physiol.* **282**, R1191–R1199 (2002). Medline

39. F. Brette, L. Sallé, C. H. Orchard, Differential modulation of L-type Ca^{2+} current by SR Ca^{2+} release at the T-tubules and surface membrane of rat ventricular myocytes. *Circ. Res.* **95**, e1–e7 (2004). doi:10.1161/01.RES.0000135547.53927.F6 Medline

40. H. Cheng, W. J. Lederer, M. B. Cannell, Calcium sparks: Elementary events underlying excitation-contraction coupling in heart muscle. *Science* **262**, 740–744 (1993). doi:10.1126/science.8235594 Medline

41. Y. K. Ju, D. G. Allen, Intracellular calcium and Na^+-Ca^{2+} exchange current in isolated toad pacemaker cells. *J. Physiol.* **508**, 153–166 (1998). doi:10.1111/j.1469-7793.1998.153br.x Medline